International Journal of Image and Data Fusion, 2015
Vol. 6, No. 3, 216–231, http://dx.doi.org/10.1080/19479832.2015.1055834

Taylor & Francis
Taylor & Francis Group

Region- and pixel-based image fusion for disaggregation of actual evapotranspiration

Fakhereh Alidoost*, M. Ali Sharifi and Alfred Stein

Faculty of Geo-information Science and Earth Observation (ITC), University of Twente, Enschede, The Netherlands

(*Received 18 February 2015; accepted 25 May 2015*)

This paper compares a region-based and a pixel-based disaggregation method used to improve obtaining actual evapotranspiration (aET) data from MODIS images. Using these methods and the relationship between different vegetation indices form Landsat-5 and aET from MODIS, a 1 km resolution aET image was disaggregated to 250 and 30 m resolutions in two steps. Disaggregated aET images were compared with aET data obtained from a Landsat-5 TM image. A sensitivity analysis using synthetic data showed the impacts of land-cover homogeneity and registration error of the input images at the three scale levels. Accuracy assessment illustrated that the region-based disaggregation method using the Normalized Difference Vegetation Index (NDVI) has a good agreement with the Landsat-5 aET, having a mean absolute error equal to 0.93 mm. This method can be powerful for improving irrigation management, as it allows to increase the spatial resolution of aET derived from remote sensing images. The study concluded that a region-based method with NDVI data performs best to disaggregate MODIS aET data.

Keywords: image fusion; disaggregation; region-based; pixel-based; evapotranspiration

1. Introduction

Image fusion is a common method used to integrate images of different resolutions. Image fusion is based on data fusion (Mangolini 1994), which can be used to increase the quality of information contained in multisource data. Image fusion, in particular, aims at disaggregating low-resolution satellite data to a higher resolution that is suitable for operational applications. It combines two or more images from the same sensor or from different sensors to obtain an image of a higher spatial and spectral resolution (Aiazzi *et al.* 2002). Images are integrated to enhance the information apparent in the images as well as to increase the reliability of the interpretation (Pohl and Van Genderen 1998). Fusion of data collected by sensors of different spatial resolutions and disaggregation techniques can either improve their visual interpretation or the quality of information derived from low spatial resolution satellite data. Image fusion methods have been mainly used to acquire finer spatial and greater spectral resolution images, whereas some were developed for obtaining higher spatial and temporal resolution images (Ha *et al.* 2013b). Image fusion, spatial sharpening, downscaling and disaggregation describe several methods to enhance the spatial resolution of the input data based on the auxiliary data (Zakšek and Oštir 2012).

*Corresponding author. Email: f.alidoost@utwente.nl

Specifically, downscaling, or disaggregation, is defined as a scaling process that converts images from a lower (coarser) resolution, s_2, to a higher (finer) resolution, s_1. Based on (Bierkens *et al*. 2000), downscaling consists of reconstructing the variation of a property at scale level s_1, given the value at the lower scale level s_2. The s_2 values may be considered as arithmetic averages of the s_1 values. Downscaling maintains the radiometric properties of the image (Luo *et al*. 2008). Bindhu *et al*. (2013) proposed non-linear disaggregation method (DisNDVI) to downscale MODerate resolution Imaging Spectroradiometer Land Surface Temperature (MODIS LST) to Landsat LST scale using NDVI and hot edge pixel model. Also, he (Bindhu and Narasimhan 2015) used Disaggregation model (DisNDVI) to disaggregate MODIS NDVI images to fine resolution based on the linear relationship between MODIS and Indian Remote-Sensing Satellite Advanced Wide Field Sensor (IRS-P6 AWiFS) NDVI. In both the techniques, it is assumed that linear or non-linear relationship between two variables is valid at different spatial scales. Silleos *et al*. (2014) used MODIS EVI (250 m) to disaggregate MODIS Leaf Area Index (LAI) (1 km) based on averaging in the moving window at finer resolution. Zheng et al. (Zheng and Zhu 2015) introduced a hybrid model based on regression and interpolation techniques to disaggregate spatially (from 25 km to 1 km) and temporally (from annual to monthly data) Tropical Rainfall Measuring Mission precipitation data.

Multi-sensor image fusion techniques play a major role in the application of remotely sensed images of different spatial and temporal resolutions in water resource management (Wu *et al*. 2012). Water requirement is an important and often complex component of water-balances in irrigated land. Irrigation water is commonly determined based on the amount of evapotranspiration (ET). ET refers to two simultaneous processes: evaporation, i.e. the loss of water from the soil surface, and transpiration being the removal of water from vegetation to the atmosphere (Allen *et al*. 1998). ET is an important factor for water circulation and energy balance between the land surface and atmosphere, as well as for decision-making related to water resource management. Actual ET (aET) is the actual amount of water consumed in the plant production system. This is distinguished from potential ET (pET), which considers the maximum transpiration capability of the plant for ET in the absence of water shortage (Pidwirny 2006). The difference between aET and pET is used to determine the irrigation water requirement by the plants. If aET and pET are estimated at a sufficient precision, then irrigation water requirement can be defined accordingly.

The Surface Energy Balance System (SEBS) is a model that has been developed for the estimation of atmospheric turbulent fluxes using satellite data in order to estimate aET (Su 2002). SEBS requires three sets of input information. The first set consists of land surface emissivity, albedo, temperature and the Normalized Difference Vegetation Index (NDVI); the second set concerns the weather variables – air pressure, humidity, temperature and wind speed – at reference height; the third set consists of downward shortwave and longwave radiations. The output resolution of SEBS is based on the spatial resolution of the thermal bands (Su 2002). These bands are not operationally available at the required resolution. Landsat provides thermal bands at a medium operational spatial resolution with a return time of 16 days. At a daily frequency, thermal bands are provided by MODIS with 1 km spatial resolution (NASA 2013). Such resolution is too coarse to make the bands suitable for operational applications.

The U.S. Geological Survey has investigated the downscaling potential of Simplified Surface Energy Balance (SSEB) aET, from 1 km to 250 m, by correlating aET with NDVI from MODIS (Haynes and Senay 2012). During disaggregation, aET can be taken from

low-resolution images, whereas its spatial distribution can be obtained from a relevant indicator, such as NDVI, at a higher resolution (Kondoh and Higuchi 2001). Relations between crop coefficients, aET and vegetation indices are showed by D'Urso *et al*. (2010), Calera and Jochum (2005), Köksala *et al*. (2010) and Runtunuwu (2007). Downscaling the spatial distribution of ET with the Surface Energy Balance Algorithm for Land (SEBAL) can best be done with regression between images (Hong *et al*. 2011). A comparison between regression-based and subtraction-based disaggregation for downscaling of MODIS images carried out by Spiliotopoulos *et al*. (2013) showed that the estimation of Landsat aET (30 m) from MODIS aET (500 m) is feasible. In these methods, however, outlier values, block effect and variability during the time are sources of uncertainty. A comparison of regression with and without intercept for estimation of monthly Landsat aET, based on annual Landsat and MODIS aET, has shown that regression-based disaggregation is not useful in a large area with dynamic changes (Singh *et al*. 2014). In these methods, the assumed linear relationship between MODIS and Landsat aET in both monthly and annual time scaling may not hold.

Advanced satellite information, in combination with Super Resolution Mapping (SRM) is able to provide reliable aET values at a high spatial resolution (Mahour *et al*. 2015). Disaggregation methods have mainly been applied to retrieve surface temperature, soil moisture and precipitation data. Limited studies have been done on disaggregation of LST and ET images. Therefore, further research is needed to evaluate and improve existing disaggregation methodologies from related disciplines to assess their applicability and accuracy for disaggregation of LST and ET images (Ha *et al*. 2013a).

In this paper, two image fusion methods are introduced and compared to predict aET with high spatial resolution (30 m). These methods are region-based and pixel-based disaggregation, which are based on the same concepts, but differ in the way that they handle the area. In the region-based model, the area is a delineated region, whereas in a pixel-based method, the area equals a pixel in the low-resolution image.

The aim of this paper is to assess the performance of region-based and pixel-based disaggregation methods to disaggregate a 1 km resolution aET image into a 250 m resolution image, and next into a 30 m resolution image. During disaggregation, aET from 1 km resolution MODIS products, 250 m resolution MODIS vegetation indices products, vegetation indices and aET from 30 m resolution Landsat-5 TM images were derived and applied. For better assessment of their performance, a sensitivity analysis was also carried out on synthetic data.

The main novelty of the paper is the combination of region-based disaggregation with image fusion. So far, disaggregation methods were mainly pixel-based, whereas traditional disaggregation methods, like regression and subtraction, apply disaggregation to the full image (Zheng and Zhu 2015). Region-based disaggregation considers regional homogeneity and its effect on the results. An additional novelty is the application that considers disaggregation of aET from a 1 km resolution into a 30 m resolution.

The structure of the paper is as follows: the concept of methods is presented in Section 2; the study area and data are introduced in Section 3; the experiments and results in Section 4; and discussion and conclusion are presented in Sections 5 and 6.

2. Methodology

During disaggregation, content information is derived from a low-resolution image, whereas the distribution of the content is derived from a relevant indicator of a high-resolution image. The assumption is that the low-resolution value is equal to the average

of high-resolution values (Bierkens *et al*. 2000). In this study, we distinguish three levels of spatial resolution: form course to fine resolutions, s_3, s_2, s_1. Region-based and pixel-based disaggregation methods are compared to show their ability to fuse different sources of data (MODIS-based aET and Landsat-based NDVI) to enhance the spatial resolution of an aET image.

2.1. Region-based and pixel-based disaggregation methods

The assumption in a region-based disaggregation method is that the average aET values for a region at level s_i is identical to average aET values of the corresponding area at level s_{i+1}. In a pixel-based disaggregation method, it is assumed that the average of aET values at level s_i is equal to the aET value of the corresponding pixel at level s_{i+1}.

For these two methods, if the spatial distribution of aET values at level $i + 1$ is known, then the disaggregated aET value at level i can be obtained by:

$$\mathrm{aET}^{(i)} = \mathrm{IM} \times \mathrm{aET}^{(i+1)} \tag{1}$$

$$\mathrm{IM} = \mathrm{VI}^{(i)}/\mathrm{VI}^{(i+1)} \tag{2}$$

where $\mathrm{aET}^{(i+1)}$ is the aET (mm) at level $i + 1$, $\mathrm{aET}^{(i)}$ is the aET (mm) at level i and IM is defined as the relative vegetation index image (dimensionless), derived from ratio of the vegetation index $\mathrm{VI}^{(\mathrm{i})}$ at level i over $\mathrm{VI}^{(i+1)}$ at level $i + 1$ (its average). aET is influenced by many parameters like the vegetation coverage, weather variables and soil conditions. In this paper, the vegetation indices are used as a proxy for ET in the region-based and pixel-based disaggregation methods. Here, it is assumed that vegetation indices can generate spatial patterns of the disaggregated ET map. The linear relationships between NDVI and the crop coefficient at different stages of crop development have been shown (Calera and Jochum 2005), and the crop coefficient is linearly related to potential ET (Allen *et al*. 1998). As vegetation indices we compared the NDVI, the Enhanced Vegetation Index (EVI) and the simple ratio (SR). These are dimensionless and defined as:

$$\mathrm{NDVI} = (\mathrm{NIR} - \mathrm{R})/(\mathrm{NIR} + \mathrm{R}) \tag{3}$$

$$\mathrm{EVI} = g \times (\mathrm{NIR} - \mathrm{R})/(\mathrm{NIR} + c_1 \times \mathrm{R} - c_2 \times \mathrm{B} + l) \tag{4}$$

$$\mathrm{SR} = \mathrm{NIR}/\mathrm{R} \tag{5}$$

where, R, NIR and B are the atmospherically corrected ground reflectance values (dimensionless) in the red, near IR and blue bands, respectively. The values of the parameters l, c_1, c_2 and g (the gain factor) are: $l = 1$, $c_1 = 6$, $c_2 = 7.5$, and $g = 2.5$, respectively, and they are dimensionless (Huete *et al*. 2002).

According to Pohl and Genderen (2013), qualitative and quantitative approaches are considered to validate image fusion results. In this study, in the absence of observed data from the field, the validity of the proposed method was analysed by comparing the disaggregated data with a Landsat-5 TM 30 m resolution aET image, indicated as $\mathrm{aET}_{\mathrm{Landsat}}$. Indicating the disaggregated ET value at each pixel with $\mathrm{aET}_{\mathrm{D}}$, we use the mean absolute error (MAE):

$$\mathrm{MAE} = (1/n) \times \sum |\mathrm{ET}_{\mathrm{Landsat}} - \mathrm{ET}_{\mathrm{D}}| \quad (6)$$

MAE is a linear and simple average of the differences and it is expressed in the same unit as the original data (for aET the unit is mm).

2.2. *Sensitivity analysis*

Below we define four experiments to disaggregate synthetic low-resolution aET to show the impact of three sources of error on the two disaggregation methods. Sources of error that we distinguish are: homogeneity of a selected region, the registration error between high- and low-resolution images and gross error in low-resolution images. A region-based method has the following advantages: the disaggregation is robust, avoids blurring effects and high sensitivity to noise and mis-registration, which are well-known problems in a pixel-based approach (Piella 2003).

In a region-based disaggregation method, the selection of a region is an important step, as it can vary from one pixel (in a pixel-based method) to a part or the whole of an image or a mosaic of several images (in a region-based method). The coefficient of variation CV = σ/μ is used as a measure of homogeneity, where μ and σ are the mean and standard deviation of the pixel values in the selected region, respectively. A low CV (CV < 0.2) among pixels in a selected region indicates a high homogeneity of the land cover. Also, disaggregation methods require precise registration of low- and high-resolution image. This is often difficult to achieve due to the large pixel size difference and mixed pixels.

To study factors affecting selection of the proper size and characteristics of a region as well as the effects of registration and gross errors on disaggregated results, four experiments have been designed using four schemes of synthetic data sets. These schemes are summarised in Table 1.

Scheme 1, the reference: the area is homogenous (CV < 0.2), and there is no registration error between low- and high-resolution images and no gross error.

Scheme 2, heterogeneity of land cover: the area is heterogeneous (CV > 0.2), and there is no registration error between low- and high-resolution images and no gross error.

Scheme 3, registration error: the area is homogenous (CV < 0.2), and there is a registration error equal to one pixel shift between low- and high-resolution images and no gross error.

Scheme 4, gross error: The area is homogenous (CV < 0.2) and there is no registration error between low- and high-resolution pixels, but there is a gross error equal to four times of the average in the low-resolution ET values.

Table 1. Four experiments have been designed to study the effect of different sources of errors on disaggregated results.

Source of error	Scheme 1; reference	Scheme 2	Scheme 3	Scheme 4
Heterogeneity of land cover	-	√	-	-
Registration error	-	-	√	-
Gross error	-	-	-	√

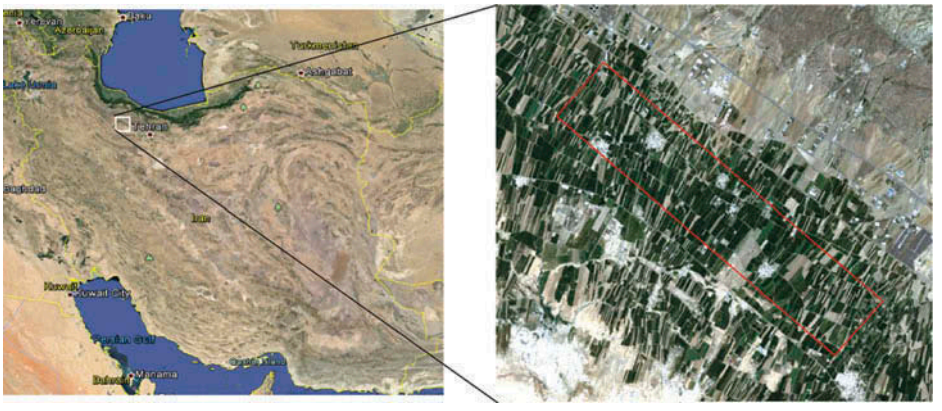

Figure 1. Study area is in Qazvin Plain in Iran. Qazvin irrigation network is composed of agricultural fields.

3. Study area and data sets

3.1. Study area

The study area is located between 50.31 N and 50.42 N and 36.03 E and 36.11 E, in the Qazvin Plane, Iran. This area covers a portion of the Qazvin irrigation network with total area of 4789×10^4 m^2, which is composed of agricultural fields dominated by wheat, maize, sorghum, alfalfa and summer crops and natural vegetation (Figure 1). This area has been the pilot for a project aiming at the development of a planning and monitoring system supporting irrigation management in Qazvin irrigation network (Sharifi 2013).

3.2. Remotely sensed data

MODIS products with 1000 m and 250 m resolution and Landsat-5 TM image with 30 m resolution are supplied. MODIS products are downloaded from the NASA Land Processes Distributed Active Archive Centre. Landsat-5 TM is downloaded from the USGS U.S. Geological Service Archive. Data sets are presented in Table 2. Due to availability of cloud-free MODIS and concurrent Landsat images, the growth season of major crops and availability of weather station data, images are selected from May 2011. MOD03 and MYD03 provide per-pixel solar/sensor zenith angle, solar/sensor zenith azimuth angle and digital elevation model values in a sequence of swath-based products at 5-minute increments. The solar zenith angle is used to calculate shortwave downward radiation. MOD11_L2 and MYD11_L2 provide per-pixel temperature and emissivity values in a

Table 2. MODIS products and Landsat data set.

MODIS products	Spatial resolution (m)	Layers	Dates
MCD43B4	1000	Reflectance (7 bands)	25 May 2011
MOD15A2	1000	LAI	25 May 2011
MOD11_L2 and MYD11_L2	1000	LST, Emissivity	25 May 2011
MOD03 and MYD03	1000	Solar/Sensor angles, Height	25 May 2011
MOD13Q1	250	NDVI, EVI, Red, IR, Blue	25 May 2011
Landsat-5 TM	30	DN (7 bands)	29 May 2011

sequence of swath-based products at 5 minute increments. MOD03 and MYD03 geo-location products were used for geo-referencing. Land surface reflectance in seven bands (MCD43B4) was used to retrieve land albedo and NDVI. Also, MOD15A2 provides 8 day LAI.

ESRI ArcGIS 10 (ESRI 2010), ENVI 4.7 (Exelisvis 2009), MATLAB R2009 b (MATLAB 2009) and ILWIS 3.8.2 (ILWIS 2007) are used to process all data for this paper.

3.3. *Synthetic data*

Synthetic data are used to explore the quality and sensitivity of the two disaggregation methods with respect to land-cover characteristics, as well as existing registration errors of different scales. Synthetic data allow the detection of possible trends in the errors that occur during disaggregation. A 160 × 160 matrix simulating high-resolution synthetic aET data of a 25 m spatial resolution (s_1) is generated by assigning a random number to each pixel location. Next, based on the derived relation between aET and NDVI (NDVI = 0.11 × aET + 0.087, R^2 = 0.53), a synthetic NDVI image is generated. This relation has been derived based on a comparison between NDVI and aET from Landsat data (Figure 2). In addition, 4 × 4, 8 × 8 and 16 × 16 low-resolution synthetic ET images of 1000, 500 and 250 m resolution were generated by averaging the high-resolution data with a pixel-size ratios of 40, 20 and 10, respectively (Figure 3). In doing so, the

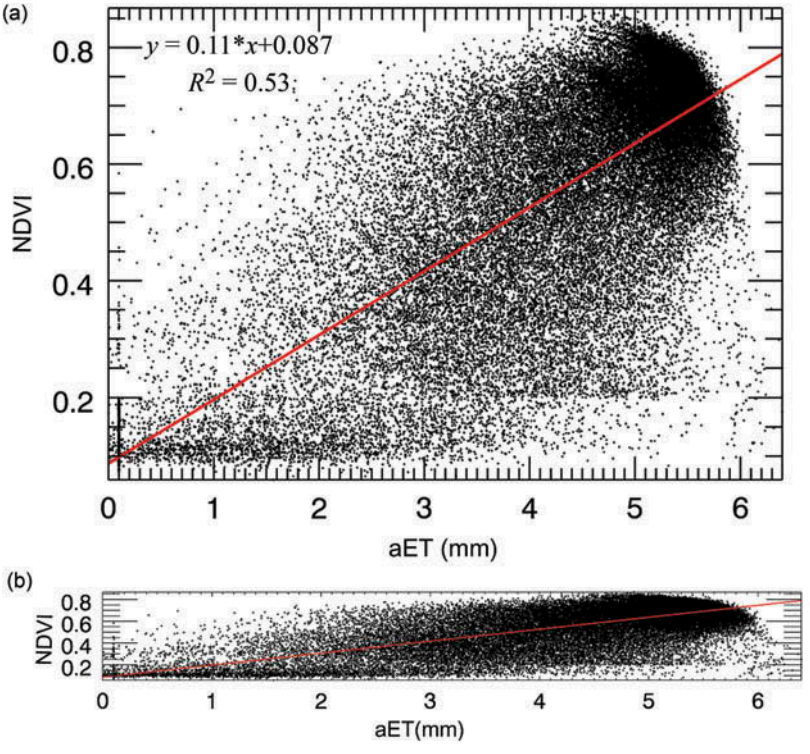

Figure 2. Relation between NDVI and aET from Landsat 5 TM data in the study area (a) anisotropic scaling; (b) isotropic scaling.

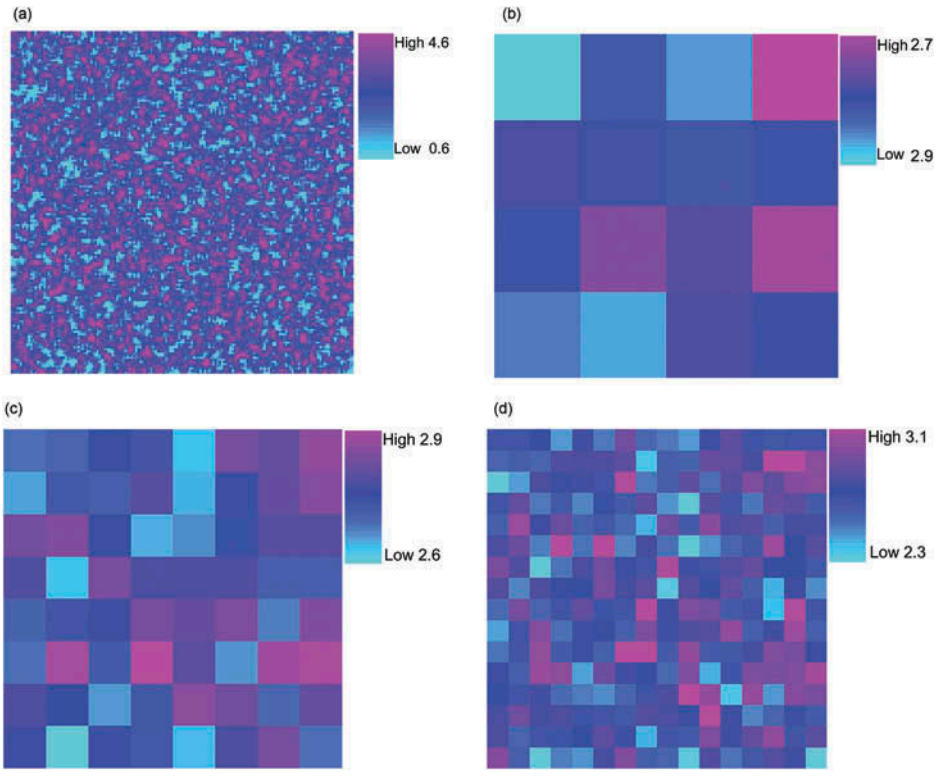

Figure 3. Synthetic data (a) aET (25 m); (b) aET (1000 m); (c) aET (500 m); (d) aET (250 m).

possibility of studying the effects of registration errors on disaggregation results was produced.

4. Results

4.1. Synthetic data

Experiment 1 shows similar results for the region-based and pixel-based methods (Table 3).

Experiment 2 showed a lower MAE for the pixel-based method than for the region-based method (Figure 4(a)). Therefore, the impact of land-cover homogeneity on the error in a region-based disaggregation method is larger than that for the pixel-based disaggregation method. When applying a pixel-based method, however, there is likely an

Table 3. MAE values in Scheme 1 (homogenous region with neither shift nor gross error) for the two methods.

MAE	
Region-based	0.09
Pixel-based	0.09

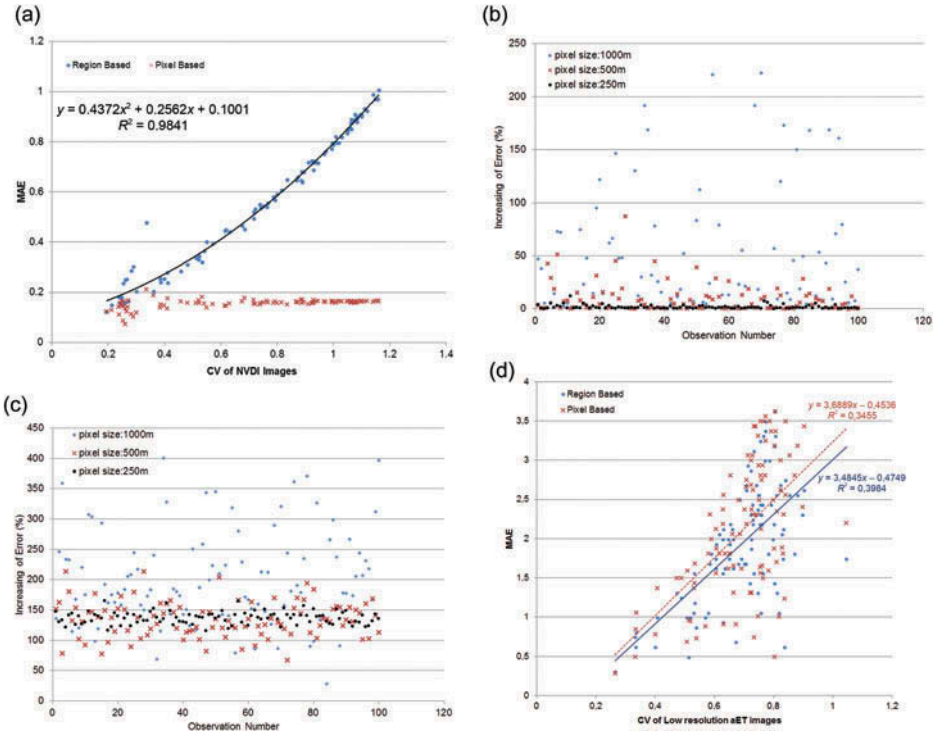

Figure 4. (a) Scheme 2 (heterogeneous region with neither shift nor gross error): The relation between homogeneity (different CVs of NDVI) and MAE; (b) Scheme 3 (homogenous region with 1 pixel shift): increased MAE due to 1 pixel shift in low-resolution image with different pixel sizes with region-based method; (c) Scheme 3: increased MAE due to 1 pixel shift in low-resolution image with different pixel sizes with pixel-based method; (d) Scheme 4: The relation between gross error (different CVs of ET) and MAE.

additional block effect which deteriorates the visual impression of the resulting image. To better understand the effect of heterogeneity of different land-cover types for the two methods, different synthetic NDVI images with different CV values reflecting the heterogeneity in the spatial distribution of different land covers were investigated with the MAE for 100 different observations (Figure 4(a)). The region-based method is more sensitive to variation in land cover, as changing CV results in changes in MAE values: $MAE = 0.437 \times CV^2 + 0.256 \times CV + 0.1$.

In Experiment 3, the increase of MAE of the region-based method (Figure 4(b)) is smaller than that of the pixel-based method (Figure 4(c)). The results indicate that the region-based method is less sensitive to registration error. This is in line with Wu *et al.* (2012), who showed that the mismatch of scales is not so critical in an area of homogeneous land use as well as with Piella (2003), who showed a region-based approach is robust to mis-registration. A plot based on the MAE and different pixel-size ratios (for 100 different observations) shows that the effect of one pixel shift in a low-resolution image is related to pixel-size ratio (Figure 4(c)). Therefore, the effect of registration error increases if the pixel-size ratio increases; when taking, for example, MODIS (250 m) as the low-resolution image and Landsat (30 m) as the high-resolution image (pixel-size ratio = 8.33), the effect of registration error as a one pixel shift on disaggregation is less

than that using a MODIS (1000 m) as the low-resolution image and Landsat (30 m) as the high-resolution image (pixel-size ratio = 33.3).

Experiment 4 shows that the effect of gross error in low-resolution aET image on the disaggregation error is larger than either homogeneity or mismatching. A regression is carried out to relate the MAE of two methods to the CV values from a low-resolution aET image (for 100 different observations) (Figure 4(d)). The region-based method apparently is less sensitive than the pixel-based method to the gross error in the low-resolution aET (region-based: MAE = 3.468 × CV – 0.475, pixel based: MAE = 3.689 × CV – 0.454).

4.2. *Remote-sensing data*

4.2.1. *Comparison of the pixel-based and region-based methods*

The two disaggregation methods were applied to a sample subset of 14 × 12 pixels from a 1000 m resolution MODIS image (s_3) in the study area. This subset corresponded to a subset of 57 × 49 pixels of 250 m resolution NDVI pixels (s_2) and to a subset of 471 × 409 pixels of 30 m resolution Landsat NDVI (s_1) pixels. For all data, a geometric correction was carried out by the suppliers, whereas the quality of geo-referencing had been checked using 1:25000 topographic maps. Thus the data were suitable for the experiment. aET at level s_3 was calculated by SEBS in ILWIS and used for disaggregation towards levels s_2 and s_1. aET at level s_1 was also calculated by SEBS in MATLAB and used for validation. The CV of the low-resolution aET and high-resolution NDVI subset was equal to 0.16 and 0.36, respectively.

According to the result of sensitivity analysis of disaggregation methods in Section 4.2.1, the method can lead to good-quality output of disaggregation, assuming there is small registration error between MODIS and Landsat-5 TM (0.5 pixel according to MODIS). Using the linear regression from Experiment 2 (Figure 4(a)), the MAE was equal to 0.25 mm, whereas using the linear regression from Experiment 4 (Figure 4(d)), MAE value of 0.08 mm can be observed for the region-based method. The aET of Landsat-5 TM is shown in Figure 5, whereas the aET values obtained from MODIS (1000 m) using SEBS (Figure 6) that was disaggregated to the aET at 30 m resolution by means of the two methods are shown in Figure 7(a) and (b). Image errors and their histograms were determined for each method (Figure 7(c),(e),(f)). The pixel-based method causes outlying aET values, i.e. aET values greater than 10 mm in the study area in approximately 0.3% of the pixels in the image. Also, the maximum and standard deviation of the errors in the pixel-based method are greater than in the region-based method. Therefore, the region-based method (MAE = 0.93 mm) performed better as compared to the pixel-based method (MAE = 1.14 mm) (Table 4).

4.2.2. *The region-based method with different vegetation indices*

To assess the impact of different vegetation indices on region-based disaggregation and also to find which one better represents the spatial patterns of the disaggregated aET map, region-based disaggregation of MODIS aET is re-examined using EVI and SR. MAE values and absolute error images were determined to do so (Figure 8). The results indicated that NDVI (MAE = 0.93 mm, Figure 7 (e)) is producing a better result than EVI (MAE = 1.21 mm, Figure 8(e)) and SR (MAE = 1.48 mm, Figure 8(f)) when disaggregating ET. SR causes outrange values of aET (aET values greater than 10 mm)

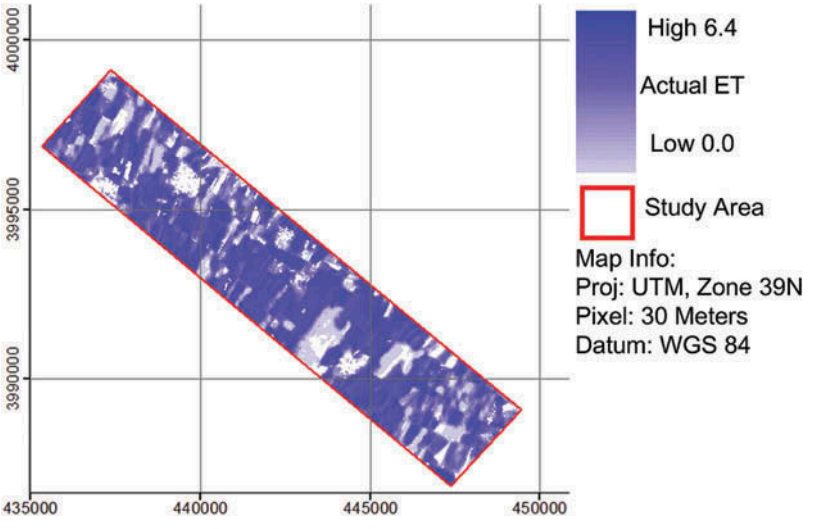

Figure 5. Actual ET from Landsat-5 TM 30 m for validation.

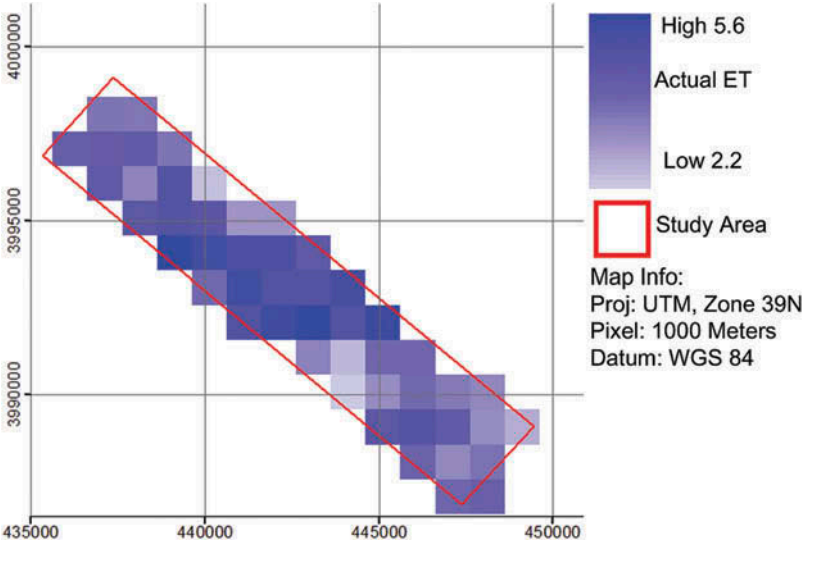

Figure 6. Actual ET image from MODIS products 1000 m (s_3).

in 1.1% of the total number of pixels in the image and EVI had a smaller MAE than SR (Table 4).

5. Discussion

Experiments with remotely sensed data showed that there is likely a block effect in the pixel-based results. This deteriorates the visual impression of the produced high-resolution images (see Figure 9). A likely cause is the land cover, as a single low-resolution pixel covers 100 ha of land, being composed of several different land uses. The pixel-based

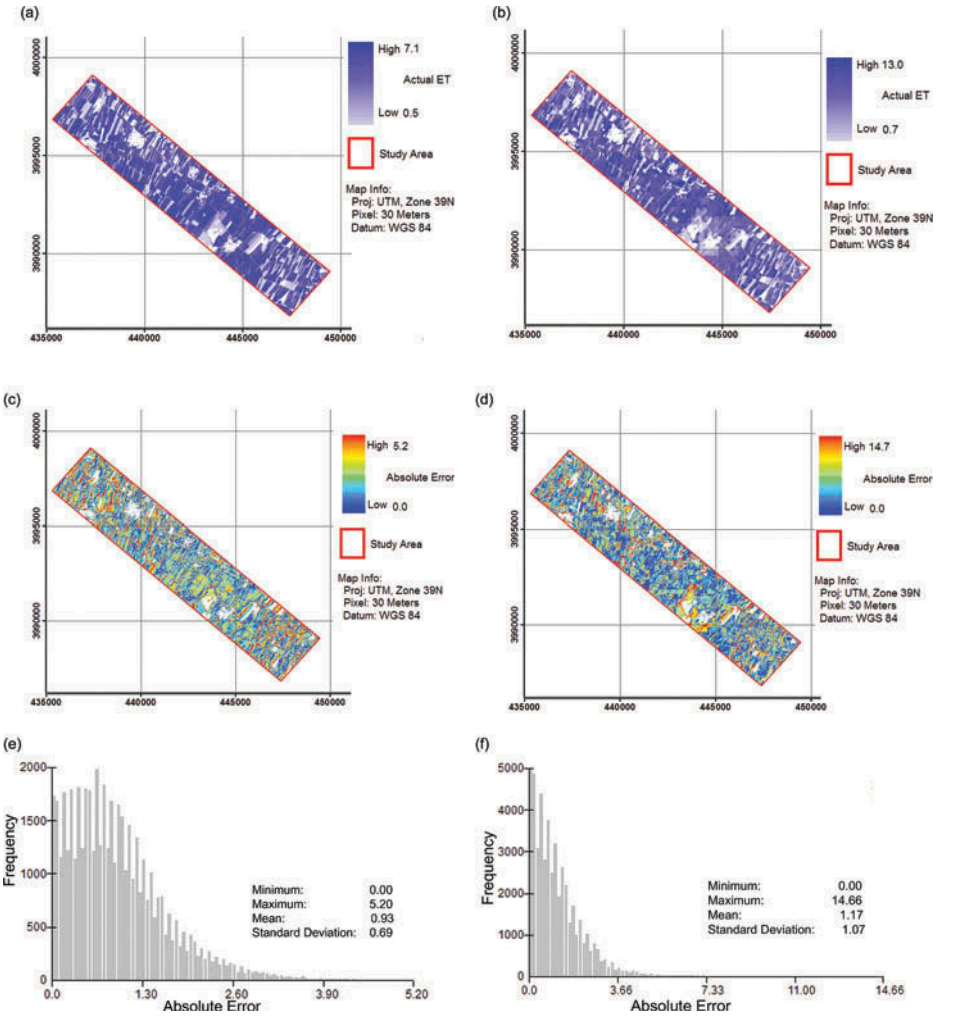

Figure 7. Actual ET (a) region-based, (b) pixel-based; Absolute error (c) region-based, (d) pixel-based; Histogram of absolute error (e) region-based, (f) pixel-based.

Table 4. MAE values (mm) with different vegetation indices in the two methods.

	NDVI	EVI	SR
Region-based	0.93	1.21	1.48
Pixel-based	1.17	-	-

method also produces outliers, which can be controlled by introducing constraints. This requires extension of the method plus some field measurements. In the region-based method the critical point is the selection of the region, which should be as homogenous as possible. In fact, the absolute point accuracy of region-based method is related to the homogeneity of selected region.

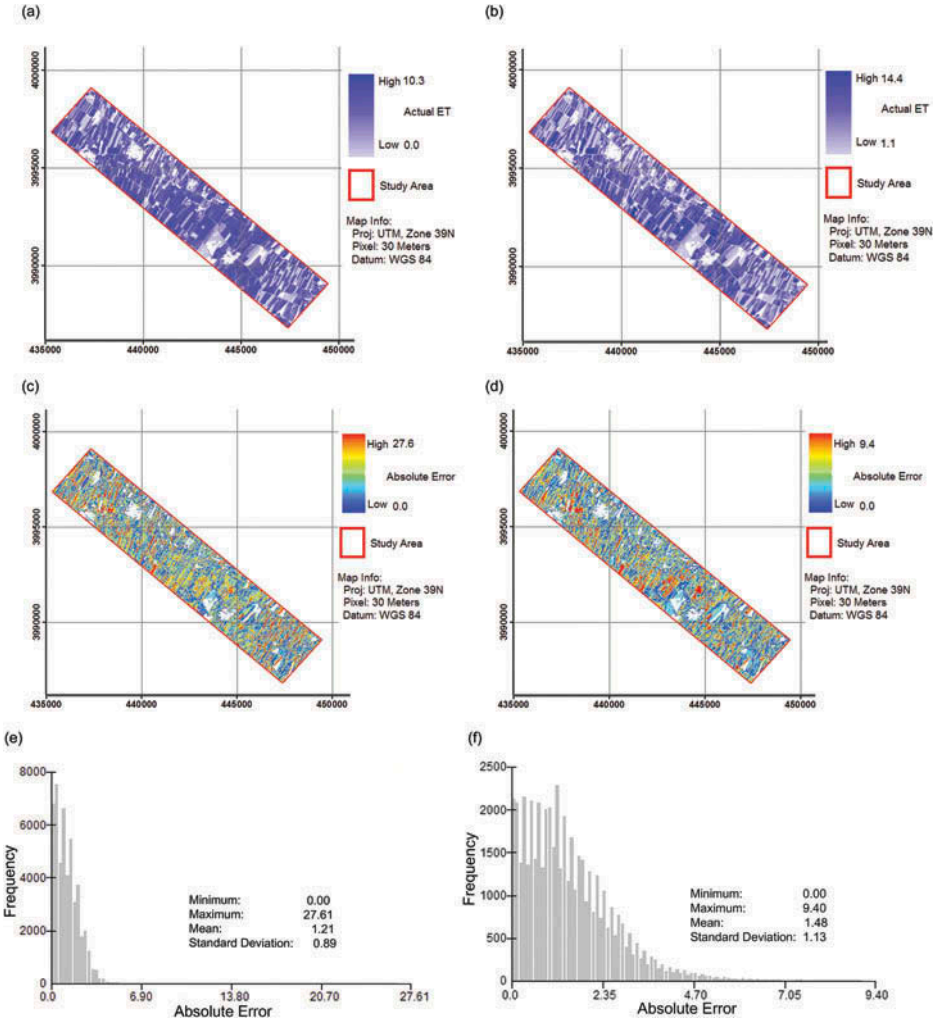

Figure 8. Region-based disaggregation results: Actual ET (a) EVI, (b) SR; Absolute error (c) EVI, (d) SR; Histogram of absolute error (e) EVI, (f) SR.

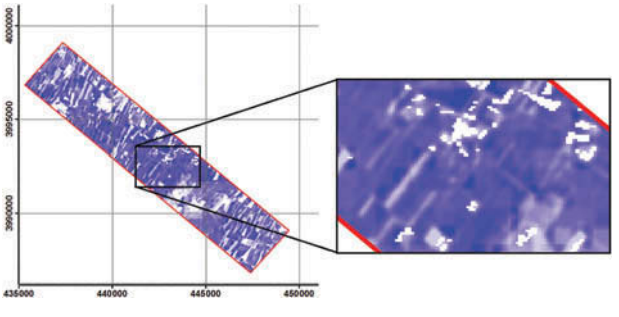

Figure 9. Block effect in the pixel-based results; the block size is equal to the size of one low-resolution pixel.

The methods were also assessed using MODIS products and Landsat-5 TM image data with different vegetation indices. On the basis of experiments, the disaggregation of MODIS aET using NDVI of higher resolution, we note that the region-based disaggregation method is performing well and can be considered as a powerful technique supporting irrigation management and crop monitoring.

Although the disaggregation methods were designed for Landsat and MODIS data, they can be applied to any two sets of image data, which fulfil the required condition. In this study, for region-based disaggregation, we have taken a large area (all the study area as one region) in the high-resolution NDVI images. This area includes different land uses and land covers that are inhomogeneous. Using small regions (parcels) or more homogenous area as regions may produce better results. As different land covers would most likely be better and can result in more precise point accuracy. Further research has to be carried out to further analyse this issue.

The basic assumption behind these methods is the close correlation between aET and vegetation indices. If this assumption in a particular cases does not hold, then results may become unreliable. As the region-based or pixel-based methods take the aET value from the aET value of the low-resolution image, using either the pixel or the region average and spatial distribution from NDVI from the higher-resolution image, then the overall values are reliable.

6. Conclusion

In this paper, two image fusion methods (region-based and pixel-based) for disaggregation of low-spatial resolution aET were suggested and compared. The methods were tested with four different schemes of synthetic data, as well as remotely sensed data derived from MODIS and Landsat-5 acquired in 2011 over Qazvin, Iran. The methods were used to combine aET derived from MODIS (1 km) and NDVI derived from Landsat-5 (30 m) to retrieve high-resolution aET image. The disaggregated high-resolution aET was evaluated by the comparison with original aET derived from SEBS algorithm using Landsat-5 products. This study shows that disaggregation using NDVI and the region-based method produces the best result.

From this study, we can conclude the following:

- The study indicated that disaggregation of aET derived from MODIS data to 30 m resolution can be accurately carried out using region-based method (better than pixel-based), despite the significant error that is inherent in some of the remotely sensed data.
- The results showed that the disaggregation works better if NDVI was deployed instead of other vegetation indices with region-based method, and there is a strong correlation between aET-based MODIS data and NDVI-based Landsat data in the same region and at the same time.
- Finally, the method can be considered universal if there exists a good correlation between the high-resolution indicator (e.g. NDVI) and the low-resolution factor (e.g. aET) that is going to be disaggregated.
- With respect to different sources of errors that are considered in the sensitivity analysis of methods with synthetic data, e.g. heterogeneity in land cover, registration error and gross error in low-resolution images, results of experiments showed that the effect of gross error in low-resolution images is greater than that of the others.

Acknowledgements

The authors wish to thank the SAJ-GIT Consulting firm for all kinds of support to carry out this study. Also, the authors would like to thank the anonymous reviewers for their comments on the manuscript.

Disclosure statement

No potential conflict of interest was reported by the authors.

References

Aiazzi, B., *et al*., 2002. Context-driven fusion of high spatial and spectral resolution images based on oversampled multiresolution analysis. *IEEE Transactions on Geoscience and Remote Sensing*, 40 (10), 2300–2312. doi:10.1109/TGRS.2002.803623

Allen, R.G., *et al*., 1998. Crop evapotranspiration-guidelines for computing crop water requirements-FAO irrigation and drainage paper 56. *FAO, Rome*, 300, 6541.

Bierkens, M.F.P., Finke, P.A., and de Willigen, P., 2000. Upscaling and downscaling methods for environmental research. In: *Developments in plant and soil sciences*. Dordrecht: Kluwer Academic.

Bindhu, V.M. and Narasimhan, B., 2015. Development of a spatio-temporal disaggregation method (DisNDVI) for generating a time series of fine resolution NDVI images. *ISPRS Journal of Photogrammetry and Remote Sensing*, 101, 57–68. doi:10.1016/j.isprsjprs.2014.12.005

Bindhu, V.M., Narasimhan, B., and Sudheer, K.P., 2013. Development and verification of a non-linear disaggregation method (NL-DisTrad) to downscale MODIS land surface temperature to the spatial scale of Landsat thermal data to estimate evapotranspiration. *Remote Sensing of Environment*, 135, 118–129. doi:10.1016/j.rse.2013.03.023

Calera, A. and Jochum, A., 2005. *DEMETER,EO Methodology Handbook*. Albacete: Universidad de Castilla-la Mancha.

D'Urso, G., *et al*., 2010. Earth observation products for operational irrigation management in the context of the PLEIADeS project. *Agricultural Water Management*, 98, 271–282. doi:10.1016/j.agwat.2010.08.020

ESRI, 2010. *ArcGIS* [online]. Redlands, CA: ESRI. Available from: http://www.esri.com/software/arcgis.

Exelisvis, 2009. *ENVI* [online]. Melbourne, FL: Exelis Visual Information Solutions. Available from: http://www.exelisvis.com/ProductsServices/ENVI/ENVI.aspx.

Ha, W., Gowda, P., and Howell, T., 2013a. A review of downscaling methods for remote sensing-based irrigation management: part I. *Irrigation Science, Springer-Verlag*, 31 (4), 20.

Ha, W., Gowda, P., and Howell, T., 2013b. A review of potential image fusion methods for remote sensing-based irrigation management: part II. *Irrigation Science, Springer-Verlag*, 31 (4), 19.

Haynes, J. and Senay, G., 2012. *Evaluation of the relation between evapotranspiration and normalized difference vegetation index for downscaling the simplified surface energy balance model*. Reston, VA: U.S. Geological Survey Scientific Investigations Report.

Hong, S., Hendrickx, J.H., and Borchers, B., 2011. Down-scaling of SEBAL derived evapotranspiration maps from MODIS (250 m) to Landsat (30 m) scales. *International Journal of Remote Sensing*, 32 (21), 6457–6477. doi:10.1080/01431161.2010.512929

Huete, A., *et al*., 2002. Overview of the radiometric and biophysical performance of the MODIS vegetation indices. *Remote Sensing of Environment*, 83 (1–2), 195–213. doi:10.1016/S0034-4257(02)00096-2

ILWIS, 2007. *ILWIS* [online]. World Institute for Conservation and Environment. Available from: http://www.ilwis.org/.

Köksala, E., *et al*., 2010. Estimation of dwarf green bean water use under semi-arid climate conditions through ground-based remote sensing techniques. *Agricultural Water Management*, 98 (2), 353–360.

Kondoh, A. and Higuchi, A., 2001. Relationship between satellite-derived spectral brightness and evapotranspiration from a grassland. *Hydrological Processes*, 15 (10), 1761–1770. doi:10.1002/(ISSN)1099-1085

Luo, Y., Trishchenko, A., and Khlopenkov, K., 2008. Developing clearsky, cloud and cloud shadow mask for producing clear-sky composites at 250-meter spatial resolution for the seven MODIS

land bands over Canada and North America. *Remote Sensing of Environment*, 112 (12), 4167–4185. doi:10.1016/j.rse.2008.06.010

Mahour, M., *et al*., 2015. Integrating Super Resolution Mapping and SEBS modeling for evapotranspiration mapping at the field scale. *Precision Agriculture*, 16. doi:10.1007/s11119-015-9395-8

Mangolini, M., 1994. *Apport de la fusion d'images satellitaires multicapteurs au niveau pixel en teledetection et photo-interpretation*. Nice: University of Nice-Sophia Antipolis.

MATLAB, 2009. *Mathworks* [online]. Natick, MA: The MathWorks. Available from: www.mathworks.com/products/matlab

NASA, 2013. *NASA* [online]. National Aeronautics and Space Administration. Available from: http://www.nasa.gov/

Pidwirny, M., 2006. Actual and potential evapotranspiration. *In*: *Fundamentals of physical geography*. 2nd ed. Kelowna: PhysicalGeography.net.

Piella, G., 2003. A general framework for multiresolution image fusion: frompixels to regions. *Information Fusion*, 4 (4), 259–280. doi:10.1016/S1566-2535(03)00046-0

Pohl, C. and Genderen, J., 2013. Remote sensing image fusion: an update in the context of digital earth. *International Journal of Digital Earth*, 7 (2), 17.

Pohl, C. and Van Genderen, J.L., 1998. Review article multisensor image fusion in remote sensing: concepts, methods and applications. *International Journal of Remote Sensing*, 19 (5), 823–854. doi:10.1080/014311698215748

Runtunuwu, E., 2007. Determination of crop coefficient using ground climatologically data and vegetation index derived from NOAA/AVHRR satellite. *Ilmu-Ilmu Pertanian Indonesia*, 9 (2), 7.

Sharifi, M., 2013. *Development of planning and monitoring system supporting irrigation mangement in the Ghazvin irrigation network*. Tehran: SAJ.

Silleos, N., *et al*., 2014, Weekly time series of LAI maps at river basin scale using MODIS satellite data. *In*: K. Perakis, ed. *1st international GEOMAPPLICA conference*, 8–11 September, Skiathos.

Singh, R., *et al*., 2014. On the downscaling of actual evapotranspiration maps based on combination of MODIS and Landsat-based actual evapotranspiration estimates. *Remote Sensing*, 6 (11), 10483–10509. doi:10.3390/rs61110483

Spiliotopoulos, M., *et al*., 2013. A spatial downscaling procedure of MODIS derived actual evapotranspiration using Landsat images at central Greece. *In*: *First international conference on remote sensing and geoinformation of the environment*. Paphos: SPIE.

Su, Z.B., 2002. The surface energy balance system (SEBS) for estimation of turbulent heat fluxes. *Hydrology and Earth System Sciences*, 6 (1), 85–100. doi:10.5194/hess-6-85-2002

Wu, B., *et al*., 2012. Validation of ETWatch using field measurements at diverse landscapes: A case study in Hai Basin of China. *Journal of Hydrology*, 436-437, 67–80. doi:10.1016/j.jhydrol.2012.02.043

Zakšek, K. and Oštir, K., 2012. Downscaling land surface temperature for urban heat island diurnal cycle analysis. *Remote Sensing of Environment*, 117 (15), 114–124. doi:10.1016/j.rse.2011.05.027

Zheng, X. and Zhu, J., 2015. A methodological approach for spatial downscaling of TRMM precipitation data in North China. *International Journal of Remote Sensing*, 36 (1), 144–169. doi:10.1080/01431161.2014.995275